

In-flight comparison of MOZAIC and POLINAT water vapor measurements

M. Helten,¹ H. G. J. Smit,¹ D. Kley,¹ J. Ovarlez,² H. Schlager,³ R. Baumann,³
U. Schumann,³ P. Nedelec,⁴ and A. Marengo⁴

Abstract. An intercomparison of airborne in situ water vapor measurements by two European research projects Measurement of Ozone and Water Vapor by Airbus In-Service Aircraft (MOZAIC) and Pollution From Aircraft Emissions in the North Atlantic Flight Corridor (POLINAT) was performed from aboard the *Airbus* (MOZAIC) and *Falcon* (POLINAT) aircraft, respectively. The intercomparison took place southwest of Ireland on September 24, 1997, at 239 hPa flight level. MOZAIC uses individually calibrated capacitive humidity sensors for the humidity measurement. POLINAT employs a cryogenic frost-point hygrometer developed for such measurements. For conversion between humidity and mixing ratio, ambient temperature and pressure measurements on board the respective aircraft are used. The *Falcon* followed the *Airbus* at a distance of 7–35 km with a time lag increasing from 30 to 160 s. The water vapor volume mixing ratio measurements in the range of 80–120 ppmv of both instruments are in excellent agreement, differing by $<\pm 5\%$, where the trajectories of both aircraft are very close. However, the relative humidity (RH) calculated from POLINAT frost-point measurements and the *Falcon* PT500 temperature sensor is up to 15% higher relative to the RH of MOZAIC. The agreement improved to within 5% when using the temperature measurement of the PT100 sensor instead of the temperature measurement of the PT500 sensor for RH determination of POLINAT.

1. Introduction

Water vapor provides 60% of the natural clear-sky greenhouse effect, more than twice that of carbon dioxide (CO₂). Water vapor is important for cloud formation and the longwave cloud forcing is also of about the same size as the clear-sky CO₂ forcing [Kiehl and Trenberth, 1997]. Moreover, water vapor enhances strongly the greenhouse effect from anthropogenic increases in atmospheric concentration of CO₂ [Möller, 1963; Manabe and Weatherald, 1967; Houghton et al., 1996]. The largest impact on radiative forcing by water vapor is expected from changes in upper tropospheric (UT) humidity [Shine and Sinha, 1991].

Harries [1997], in considering the combined uncertainties in UT water vapor concentration and spectroscopic properties of water vapor in the far infrared, stated that the concentration of humidity, particularly in the UT, may need to be known with an accuracy in the range of 3–10% if uncertainties of the order of the radiative effect of CO₂ doubling are to be avoided. An accuracy requirement of 3–10% places very high demands on any measurement system. In the case of UT water vapor this has not been

achieved so far by operational sensors on radiosondes or satellites. Research instrumentation, such as the frost-point hygrometer [Oltmans et al., 1985; Ovarlez, 1991] or the Lyman α fluorescence hygrometer [Kley and Stone, 1978] possess the required accuracy, in principle. However, even these high quality instruments have been shown to differ by roughly 10% for stratospheric conditions over the years.

The cause of the discrepancy is not known at present. Standard meteorological radio-sondes use capacitive sensors routinely. In the past the data provided by such sondes were often found not to be reliable at altitudes above a pressure level of ~500 hPa and at temperatures below -30°C [Elliott and Gaffen, 1991; Leiterer et al., 1997]. Measurements with previously available capacitive humidity sensors on research aircraft also showed large discrepancies compared to frost-point hygrometers at water vapor concentrations below ~0.1 g kg⁻¹ (volume mixing ratio 160 ppmv) [Ström et al., 1994].

In this paper we compare the in-flight performance of the MOZAIC water vapor sensors on a scheduled passenger aircraft with state-of-the-art frost-point hygrometer instrumentation on a research aircraft. Two European research projects, Measurement of Ozone and Water Vapor by Airbus In-Service Aircraft (MOZAIC) and Pollution From Aircraft Emissions in the North Atlantic Flight Corridor (POLINAT), aim at tropospheric water vapor measurements of known precision and accuracy together with other air constituents. To evaluate the quality of the water vapor data sets of both projects, an in-flight intercomparison of the humidity measurements was performed.

Within the MOZAIC project the large-scale distribution of tropospheric water vapor and ozone are measured onboard five Airbus A340 aircraft during scheduled flights operated by civil airlines [Marengo et al., 1998]. Each aircraft collects data up to 500 hours per month. The flights cover parts of both hemispheres and deliver measurements that sufficiently cover time and space

¹Institut für Chemie der Belasteten Atmosphäre, Forschungszentrum Jülich, D-52425-Jülich, Germany.

²Laboratoire de Météorologie Dynamique, Centre Nationale de la Recherche Scientifique, Palaiseau, France.

³Deutsches Zentrum für Luft- und Raumfahrt (DLR), Institut für Physik der Atmosphäre, Oberpfaffenhofen, Germany.

⁴Laboratoire d'Aérodynamique, Centre National de la Recherche Scientifique, Toulouse, France.

to set up climatological data sets of tropospheric water vapor at cruise altitudes (9–13 km) and also climatological water vapor altitude distributions from ascents and descents near airports. The data serve the study of dynamical and chemical processes [e.g., Gierens *et al.*, 1997] and the validation of chemical and transport models for the assessment of human impact, particularly the effects of air traffic.

The project POLINAT aims at the determination of the relative contribution from air traffic exhaust emissions to the composition of the lower stratosphere and upper troposphere at altitudes between 9 and 13 km within and near the flight corridor over the North Atlantic using airborne observations [Schlager *et al.*, 1997; Schumann, 1997]. During dedicated flights of the project, water vapor, ozone, NO_x, NO_y, SO_x, CO₂, HNO₃, HNO₂, and particulates are measured. The flights are scheduled on the basis of meteorological and chemical forecasts and known distribution of air traffic. The POLINAT water vapor frost-point measurements presented here were made by Laboratoire de Météorologie Dynamique (LMD) aboard the *Falcon* research aircraft of Deutsches Zentrum für Luft- und Raumfahrt (DLR).

2. MOZAIC Equipment

Relative humidity and temperature are measured in situ with an airborne sensing device AD-PS2 (Aerodata, Braunschweig, Germany) mounted in an appropriate housing (Model 102 BX, Rosemount Inc., Aerospace Division, United States) [Helten *et al.*, 1998]. The humidity sensor is a capacitive sensor with a hydroactive polymer film as the dielectric whose capacitance depends on the relative humidity. The temperature sensor, a platinum resistance sensor (PT100), is mounted parallel to the humidity sensor near its sensing surface for the direct measurement of the temperature. The housing with both sensors is positioned outside the fuselage, 7 m behind the aircraft nose on the left side just below the cockpit. The air entering the housing is subject to adiabatic compression by the strong speed reduction in the inlet part of the housing and leads to a significant temperature increase of the air sampled by the sensor of ~30°C in the present case.

The temperature of the ambient air, called static air temperature (SAT), can be computed from the air temperature measured inside the housing, called total recovery temperature (TRT), if the air speed of the aircraft is known [Helten *et al.*, 1998]. The relative humidity measured inside the sensor housing, called RH_D, is much lower than the ambient relative humidity, called static relative humidity (RH_S), which has to be determined. On the MOZAIC aircraft, two independent temperature measurement systems are operated; one is a PT500 sensor, the usual aircraft equipment, and the other is the MOZAIC temperature sensor, a PT100. The temperature sensors are located in separate housings (Rosemount Model 102). The standard instrument is operated with deicing on; the MOZAIC sensor is operated without deicing. Both measurements are independently operated and evaluated with their own algorithms. The temperature uncertainty of both systems is 2σ = ±0.5 K [Helten *et al.*, 1998].

For all computations of water vapor data we follow the Goff and Gratch [1946] formulation of saturation water vapor pressure over a plane surface of pure water or ice recommended by the World Meteorological Organization (WMO) [1983] and adapted to the international temperature scale 1990 (ITS-90) [Sonntag, 1994]:

$$E(T) = \exp\left[\frac{a}{T} + b + cT + dT^2 + e \ln(T)\right] \quad (1)$$

where E is in pascals and T is in degrees Kelvin. For E over water, called E_w , the constants are $a = -6096.9385$, $b = 21.2409642$, $c = -2.711193E-2$, $d = 1.673952E-5$, and $e = 2.433502$. For E over ice, called E_i , the constants are $a = -6024.5282$, $b = 29.32707$, $c = 1.0613868E-2$, $d = -1.3198825E-5$, and $e = -0.49382577$.

Relative humidities are always expressed with respect to a plane surface of pure water in this paper. The ambient humidity RH_S is computed with the formula

$$RH_S = RH_D \cdot \left(\frac{SAT}{TRT}\right)^{\frac{c_p}{c_p - c_v}} \cdot \frac{E_w(TRT)}{E_w(SAT)}, \quad (2)$$

where c_p (= 1005 J kg⁻¹ K⁻¹) and c_v (= 717 J kg⁻¹ K⁻¹) are the specific heats of dry air at constant pressure and volume, respectively.

The water vapor partial pressure P_w is given by

$$P_w = RH_S \cdot E_w(SAT) \cdot 10^{-2}.$$

The water vapor (H₂O) volume mixing ratio is derived from

$$\mu_{H_2O} = \frac{P_w}{P - P_w} \quad (3)$$

if P is given in pascals. For upper tropospheric conditions, P_w is much smaller than P so that μ_{H_2O} can be expressed as

$$\mu_{H_2O} = \frac{P_w}{P}. \quad (4)$$

The humidity sensors are normally changed each month and calibrated in the laboratory before installation and after deinstallation. The mean of the preflight and postflight calibration coefficients of each flight period are used to evaluate the measurements. The differences between both sets of these calibration coefficients give the main contribution to the uncertainty of the measurement [Helten *et al.*, 1998].

The specific MOZAIC aircraft used for the comparison with POLINAT was arbitrarily selected during the course of the experiment. The humidity sensor on this aircraft was not specially selected i.e., just the routine monthly changed out (installation on September 16, 1997, and removal on October 10, 1997). Two calibration coefficients, slope a and offset b , for three different temperatures are determined by the preflight and postflight calibration. For the sensor SN683108/010 used here the differences can be compared with mean and standard deviation of sensors used between January 1995 and January 1997 in MOZAIC (Table 1). The calibrated value of the humidity sensor RH_{cal} is computed from the measured sensor reading RH_{uncal} using the calibration coefficients a and b by formula

$$RH_{cal} = a + b \cdot RH_{uncal}. \quad (5)$$

Sensor SN683108/010 is within 1 standard deviation of the mean for the temperatures -20° and -30°C. For -40°C it is only within more than 2 standard deviations of the mean. The differences between both calibrations are the main contribution to the uncertainty. The measurements presented here were performed at sensor temperatures between -22.4° and -25.0°C. Therefore only the calibration coefficients at -20° and -30°C are of importance for this intercomparison. The uncertainty of the MOZAIC measurements in this intercomparison is therefore representative of the uncertainty of the MOZAIC data in total. Typical accuracy values of RH and water vapor volume mixing ratios are 4.3% RH and 7.5 ppmv for the conditions of the present flight. The 2σ uncertainty of the pressure measurement is ±0.5 hPa.

Table 1. Mean Differences of Calibration Coefficients a and b Between Preflight and Postflight Calibrations at Three Calibration Temperature Levels and Standard Deviation of Sensors Used Between January 1995 and January 1997 Compared With Sensor 683108/010 Used in This Intercomparison

	-20°C			-30°C			-40°C		
	Samples	$(a_2 - a_1)$	$(b_2 - b_1)$	Samples	$(a_2 - a_1)$	$(b_2 - b_1)$	Samples	$(a_2 - a_1)$	$(b_2 - b_1)$
Mean	56	-0.19	-0.01	59	-0.26	0.011	47	-0.31	0.02
Standard deviation	56	0.33	0.08	59	0.42	0.072	47	0.49	0.11
Sensor	1	-0.03	-0.08	1	0.05	0.015	1	0.75	0.21
	683108/010								

Calibration coefficient a equals the offset in percent relative humidity, and calibration coefficient b equals slope (see equation (5)).

3. POLINAT Equipment

The water vapor measurements in POLINAT are performed with a cryogenic frost-point hygrometer [Ovarlez and Velthoven, 1997]. The ambient air flows through an air inlet system (a modified Rosemount temperature housing model 102) to the hygrometer inside the aircraft, driven by the pressure difference between inlet and outlet. The air pressure is measured immediately at the sensor head of the hygrometer, called P_H , with an uncertainty $2\sigma = \pm 0.1$ hPa. The hygrometer measures the frost-point temperature T_F with an uncertainty $2\sigma = \pm 0.3$ °C for the frost-point range of -10° to -75° C in this comparison.

The water vapor volume mixing ratio is the ratio between water vapor saturation pressure over ice at the frost-point temperature T_F and the air pressure P_H measured by the hygrometer. Hence it is computed from

$$\mu_{\text{H}_2\text{O}} = \frac{E(T_F)}{P_H} \quad (6)$$

using $E(T)$ as given in (1). The relative humidity with respect to water RH can be calculated by

$$\text{RH} = \frac{E(T_F)}{E_w(\text{SAT})} \cdot \frac{P}{P_H} \cdot 100 = \mu_{\text{H}_2\text{O}} \cdot \frac{P}{E_w(\text{SAT})} \cdot 100. \quad (7)$$

P is the ambient air pressure. RH is in percent.

SAT, the ambient static air temperature, is measured onboard the *Falcon* research aircraft with two platinum resistance thermometers. One sensor has an open-wire sensing element (PT100), and the other one has an encapsulated sensor element (PT500). They are operated in two sensor housings (Rosemount Model 102) symmetrically mounted to both sides of the aircraft nose. The air entering the temperature housings is subjected to the adiabatic compression in the same way as described for the MOZAIC equipment. At the mean air speed of the *Falcon* during the intercomparison of 233 m s^{-1} the temperature increase was $\sim 27^\circ\text{C}$. Both temperature sensors were operated with its deicing facility on, which increased the temperature of the PT500 by ~ 0.8 K and of the PT100 by ~ 0.15 K (Figure 1). Therefore the temperature measurements have been corrected for this effect. These corrections were determined as a function of a nondimensional parameter Z (see Figure 1) by earlier experiments comparing measurements with and without deicing switched on several times along horizontal flights in calm air relative to a third temperature sensor without deicing onboard the same aircraft. The standard heating correction given by the manufacturer turned out to be in-

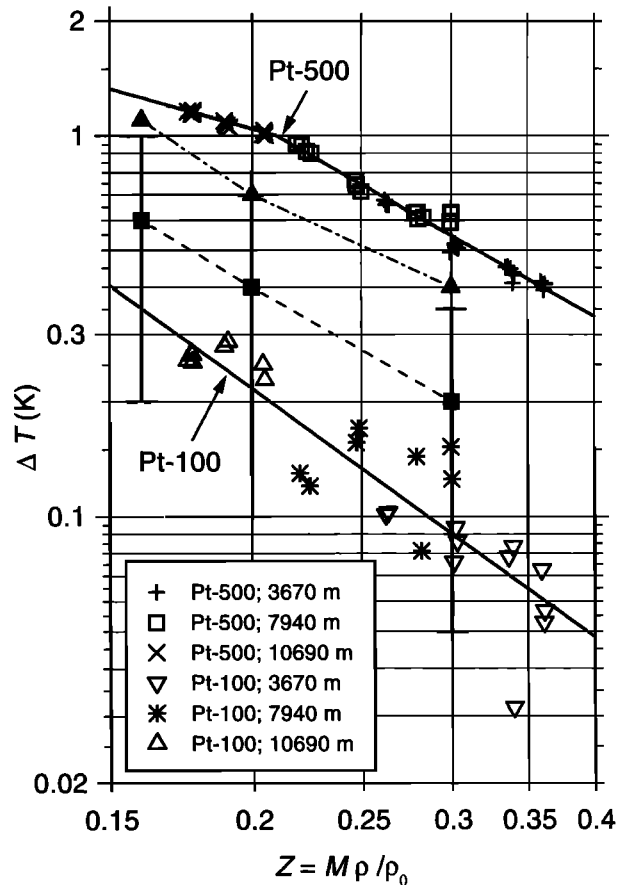


Figure 1. Temperature increment ΔT of the *Falcon* sensor temperature due to deicing heating versus the nondimensional parameter Z depending on Mach number M and ambient air density ρ . Here ρ_0 is the standard air density at sea level. The symbols indicate measured values at three different altitudes and for three different aircraft speeds for the Rosemount temperature sensor types PT100 and PT500. The solid curves indicate the fit as used for the present study. The curves connecting three data points, with error bars show the values provided by the manufacturer (dashed curve for one sensor element and dash-dotted curve for two sensor elements in one housing; the present measurements have been performed with one sensor element per housing). The present measurements were performed for $Z = 0.24$.

sufficient. Therefore the temperature measurements have been corrected for this effect. The total uncertainty of the air temperature measurements can be estimated to ± 0.5 K [Quante *et al.*, 1996]. During the POLINAT measurement period of September and October 1997, which includes the measurement event described in this paper, the PT500 sensor was used and compared also with in-flight measurements onboard a U.K. C-130 research aircraft of other research partners with deviations of 0.1 K in the mean (<0.5 K in the signals; the details of these comparisons are to be documented elsewhere). The ambient static air pressure P is measured with an uncertainty $2\sigma = \pm 0.5$ hPa.

4. Measurements and Results

The in situ intercomparison took place southwest of Ireland in the Shannon radar control zone on September 24, 1997. The POLINAT team received information on the scheduled flights (departure airport and time and flight route) for 4 of the 5 MOZAIC aircraft on a daily basis by the airlines involved. After selection of the MOZAIC flight for the intercomparison the actual departure time and the expected arrival time in the Shannon radar zone were provided by the pilot of the MOZAIC aircraft after the take off and then again 3 hours before the intercomparison. The POLINAT aircraft (*Falcon*) waited in the radar control

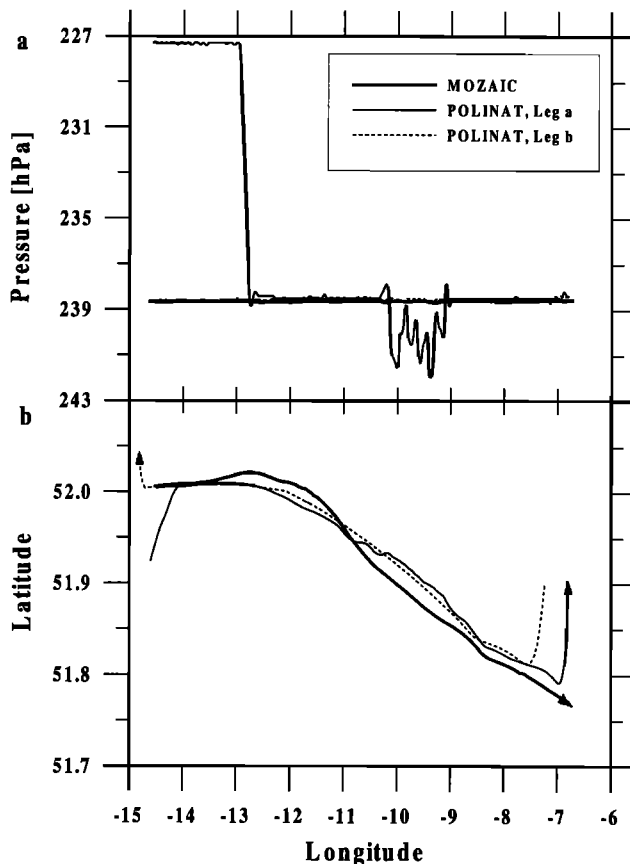


Figure 2. (a) Pressure and (b) latitude of Measurement of Ozone and Water Vapor by Airbus In-Service Aircraft (MOZAIC) and Pollution From Aircraft Emissions in the North Atlantic Corridor (POLINAT) aircraft as a function of longitude. The flight directions of the aircraft are indicated by arrows at the end of each flight leg.

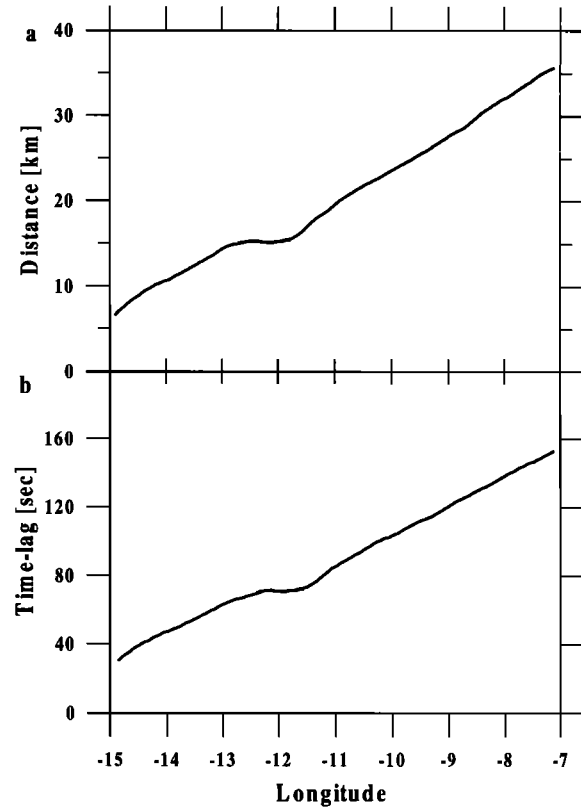


Figure 3. (a) Distance and (b) time lag between POLINAT and MOZAIC aircraft as a function of longitude.

zone in a 300 m higher flight level for the arrival of the MOZAIC aircraft (*Airbus*), which started from New York bound for Frankfurt. When the *Airbus* reached the operation region of the POLINAT aircraft at 6.40 UT, the *Falcon* followed the *Airbus*, first descending to the same flight level (239 hPa) and then following as close as allowed by air traffic control (Figure 2). The *Falcon* approached the course of the *Airbus* at -14° longitude and followed until -7° longitude. We will call this part of the *Falcon* flight leg a. When the *Falcon* reached -7° longitude, it turned and followed the course of leg a back in order to investigate the homogeneity of the H₂O field. This flight section will be called leg b. During the intercomparison the pressure differences between the aircraft were smaller than 0.2 hPa with the exception of the period between -10.4° and -9.0° longitude during leg a, where the *Falcon* aircraft descended to the contrail of the *Airbus* for exhaust plume measurements, to a maximum of 90 m below the course of the *Airbus*. This pressure difference and the uncertainties of both pressure measurements imply a relative uncertainty in altitude measurement of ± 25 m (2σ). During flight leg a the distances in time and space between the *Airbus* and the *Falcon* increased from 30 to 160 s corresponding to 7 and 35 km (Figure 3).

During flight leg a the *Airbus* trail was clearly visible as a contrail sinking down to ~ 50 m below the *Airbus* flight track. Plate 1 shows the view from the *Falcon* window flying into the sun with the contrail of the *Airbus* clearly visible below and to the right of the nose boom of the *Falcon*. Above the *Falcon*, a further contrail from another airliner is visible. This and the clouds visible below the flight track indicate a rather large relative humidity of the ambient air. The presence of the contrail was to be expected because the ambient temperature (below -52°C)



Plate 1. Photo taken by the *Falcon* pilot when following the *Airbus*, which left a pair of contrails, one for each side of the aircraft, with wavy structures indicating a Crow instability, along flight leg a, section A.

was below the threshold temperature for contrail formation ($\approx -51.2^{\circ}\text{C}$) according to the Schmidt/Appleman criterion for the present conditions (ambient pressure of 238.4 hPa, water vapor emission index of 1.26, and overall efficiency of propulsion of the aircraft of ~ 0.33) even if the ambient air were totally dry [Schumann, 1996]. The *Falcon* instruments sampled about the same air parcels as the *Airbus* instrument by following the contrail. However, the *Falcon* flew above the contrail (at the same flight level as the *Airbus*) and at the upwind side of the *Airbus* track with some stagger in order to avoid pollution of the sample air by the exhaust of the *Airbus*. Assuming isobaric transport, we computed the dislocation of the *Airbus* trail by the horizontal wind until the POLINAT aircraft reached the same longitude with the time distance between both aircraft, using zonal and meridional wind components measured by *Airbus* and *Falcon* (Figure 4). For the computation of the dislocation of the *Airbus* trail we took the changes of the wind components, measured in three different time periods, into account. The result shows that the separation of MOZAIC and POLINAT aircraft courses between -10.4° and -7.0° longitude is of the order of a few hundred meters with the exception of the *Falcon* measurements in the contrail (Figure 5), if the dislocation of the air sampled by MOZAIC by the horizontal wind is taken into account. Even for the beginning of the intercomparison at -13° longitude, the distances are smaller than 5 km. To simplify further discussion of the results, we have divided leg a into three sections. Section A is the period where the *Falcon* approached the *Airbus* course, section B designates the excursion of the *Falcon* to the *Airbus* contrail; and section C marks the closest approach of the aircraft tracks. The horizontal wind component measurements of both aircraft, meridional and

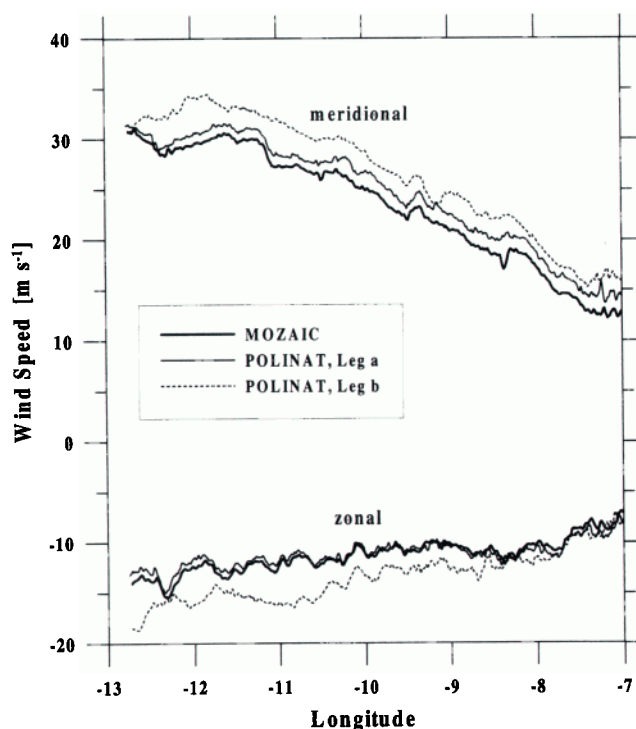


Figure 4. (top) Meridional and (bottom) zonal wind components as a function of longitude measured by the MOZAIC (thick curve) and the POLINAT (thin curves) aircraft on flight legs a and b.

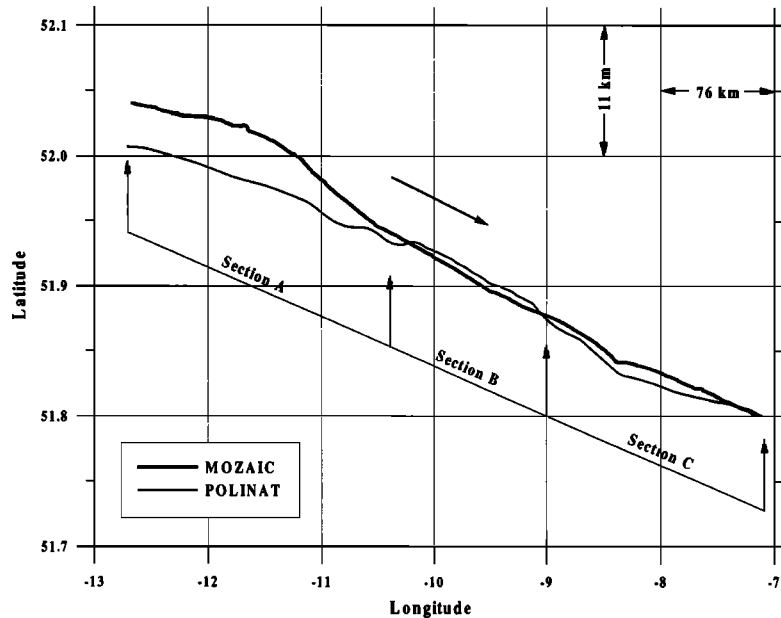


Figure 5. Flight track of the POLINAT aircraft (thin curve) compared with the MOZAIC aircraft (thick curve) flight track shifted with the horizontal wind during the period until the POLINAT aircraft reached the same longitude. The shift was computed using the measured horizontal wind and assuming isobaric transport. The different parts of the intercomparison are marked as sections A, B, and C with arrows.

zonal, show excellent agreement, reproducing also mesoscale structures (Figure 4). The meridional wind increased markedly during the experiment, as a comparison of the MOZAIC and two POLINAT measurements over a time of slightly more than one hour show. On flight leg b the *Falcon* measured stronger zonal winds for longitudes west of -8° .

Both aircraft measured SAT with two systems each, the *Airbus* with its own (PT500) and with the MOZAIC system (PT100) and the *Falcon* with a PT100 sensor and a PT500 sensor. All four sensors are mounted in separate Rosemount Model 102 housings.

For section C of the intercomparison the differences between MOZAIC PT100 and POLINAT temperatures are nearly constant, 0.64°C for the POLINAT PT500 and 0.26°C for the POLINAT PT100 (Figure 6). Part of the temperature differences may originate from uncertainties in the measured flight altitudes of the two aircraft in a vertically inhomogeneous atmosphere. For a local vertical temperature gradient of, for example 4 K km^{-1} , the uncertainty of the relative flight altitude ($\pm 25\text{ m}$) would cause a temperature difference of $\pm 0.1\text{ K}$. The differences change abruptly in section B because of the altitude gradient of the tem-

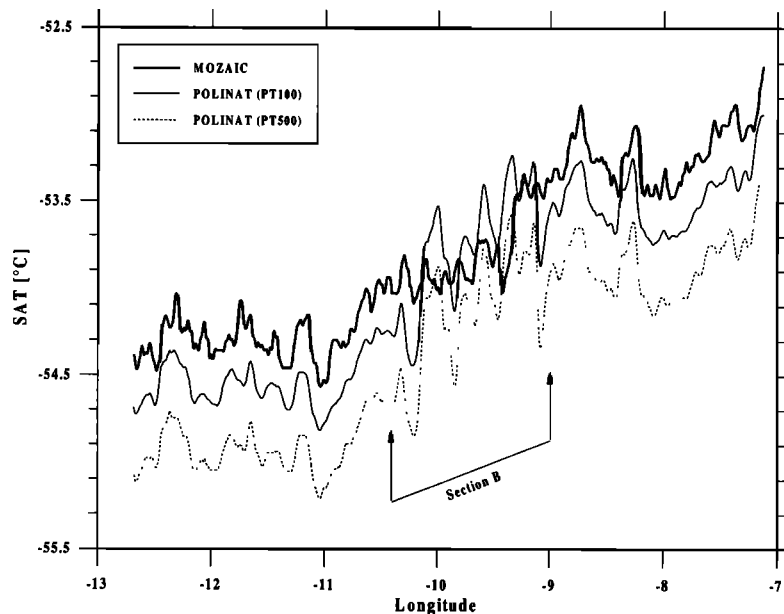


Figure 6. Static air temperature (SAT) measured by MOZAIC (thick curve) and PT100 sensor (thin curve) and PT500 sensor (dotted curve) of POLINAT as a function of longitude. The data are displayed as an average over 15 s. Section B, the excursion of *Falcon* to the *Airbus* contrail, is marked with arrows.

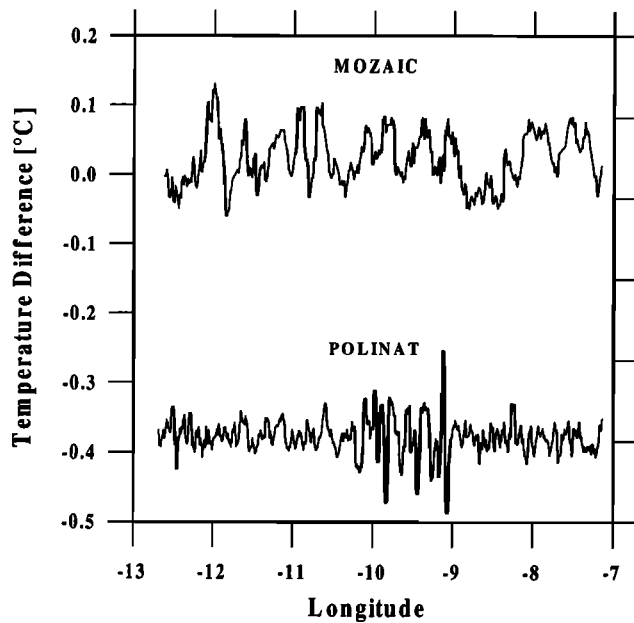


Figure 7. Static air temperature (SAT) differences between (top) both MOZAIC sensors and (bottom) both POLINAT sensors (bottom) as a function of longitude.

perature and follow the features of the POLINAT altitude profile, where the *Falcon* made excursions to lower altitudes (Figure 3). Here the structures in the MOZAIC temperature measurements are different from the POLINAT measurements. Structures in the different temperature measurements are strongly correlated in sections A and C. The measurement with the *Airbus* sensor, plotted as difference to the MOZAIC sensor in Figure 7, is within $\pm 0.15^\circ\text{C}$ of the MOZAIC sensor, showing in the mean no bias over the whole flight. Both POLINAT temperature sensors show SAT values lower than the MOZAIC measurements, while they are running quite precisely in parallel with a mean difference of $-0.4^\circ \pm 0.1^\circ\text{C}$ between PT500 and PT100 (Figure 7).

All temperature measurements are nevertheless within the quoted uncertainties of $\pm 0.5^\circ\text{C}$ and in good agreement with each other. The constant lower measurement of the POLINAT PT500 is pointing to a potential systematic error, possibly due to two reasons. First, the temperature difference due to the dynamic heating calculated with the algorithm provided by the manufacturer for both POLINAT sensors might deviate from the actual value. Second, the deicing correction might be nonoptimal because it is based on previous measurements for *Falcon* speeds between 180 and 210 m s^{-1} but used for the rather large *Falcon* speed of 233 m s^{-1} ($Z = 0.24$, see Figure 1) in this case. The use of different interpolations could imply slightly different corrections. The *Airbus* temperature measurement was evaluated with the standard correction of the manufacturer (which does not need to be optimal), while the MOZAIC sensor housing was not heated during this flight. Therefore MOZAIC temperature measurements have not been corrected for deicing.

The water vapor volume mixing ratio reveals excellent agreement in section C of the intercomparison, where the trajectories of both aircraft were closest (Figure 8). Even mesoscale structures of the water vapor volume mixing ratio are nicely reproduced. Section B, the excursion of the *Falcon* to the contrail, shows H₂O mixing ratios significantly higher than the MOZAIC measurement. Local increases in H₂O mixing ratio of the order 3 ppmv are to be expected in aircraft plumes of 100 s age [Schumann *et al.*, 1998]. Hence part of the fine structures here are caused by the water vapor injection of the *Airbus* engines.

The 1σ uncertainties of the measurements are plotted as error bars. They were computed by error propagation from (4) and (6) with the uncertainties of the measured parameters SAT , T_F , P , and P_H quoted earlier. Not included in the calculation are the uncertainties of the water vapor saturation pressure formula (1) itself.

Strong changes of the water vapor volume mixing ratio are detected faster by the POLINAT system because of the shorter response time of the frost-point instrument (typically a few seconds) compared to the MOZAIC sensor (typically more of the order of 20 s at the prevailing TRT in this altitude ($\approx -24^\circ\text{C}$)). A shift by 15 s ($\sim 3.4\text{ km}$) of the MOZAIC measurements relative to

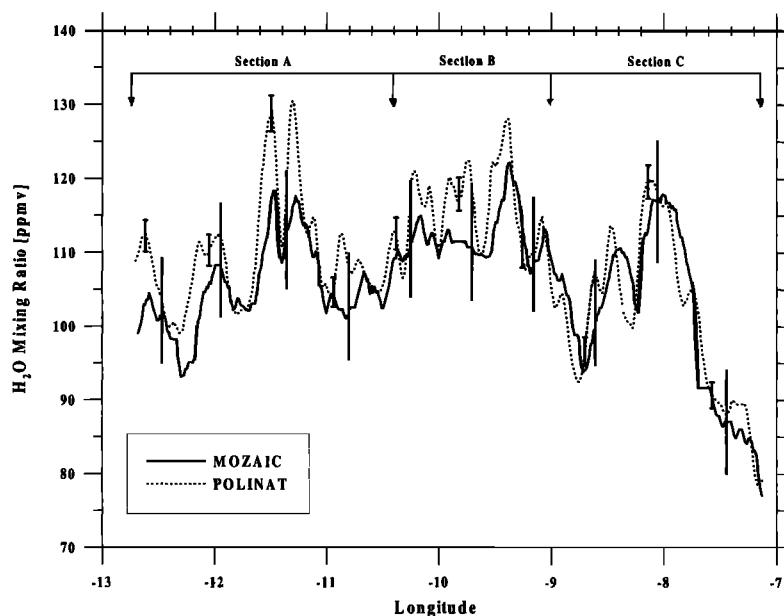


Figure 8. MOZAIC (solid curve) and POLINAT (dashed curve) water vapor volume mixing ratio as a function of longitude. The uncertainties of both measurements are plotted as error bars.

the POLINAT measurements enhances the coincidence of all structures of both measurements between -13° and -7° longitude (Figure 9). This indicates some deviation in the position measurements used or possibly different response times of the instruments onboard the two aircraft. The dislocation of the *Airbus* trail by the horizontal wind can account for only a few percent of this deviation. The relative deviation of the water vapor mixing ratios is within $\pm 5\%$ for section C with the exception of the strong decrease in water vapor concentration at -8° longitude, where the MOZAIC measurement drops much faster. That happens in a region with a strong RH gradient, where the time delay between both measurements is a maximum (~ 160 s) and the POLINAT measurement later on leg b at this position showed a strong change of the water vapor mixing ratio within 2.5 min (see Figure 11 and its discussion later). Therefore a change of the water vapor distribution could have contributed to the larger deviation. In section B a positive relative deviation of up to 10% relative to the MOZAIC measurement may be caused partly by the water vapor injection of the *Airbus*. The structures of both measurements in section A are similar, and the POLINAT values are up to 14% higher than the MOZAIC measurement. This could be partly due to the gradient of the water vapor distribution since the flight trajectories differ here up to 5 km in latitudinal direction.

The relative humidity RH is shown in Figure 10b plotted against the longitude without time lag. The RH values vary between ~ 40 and 80%, clearly exceeding ice saturation (58.2% for

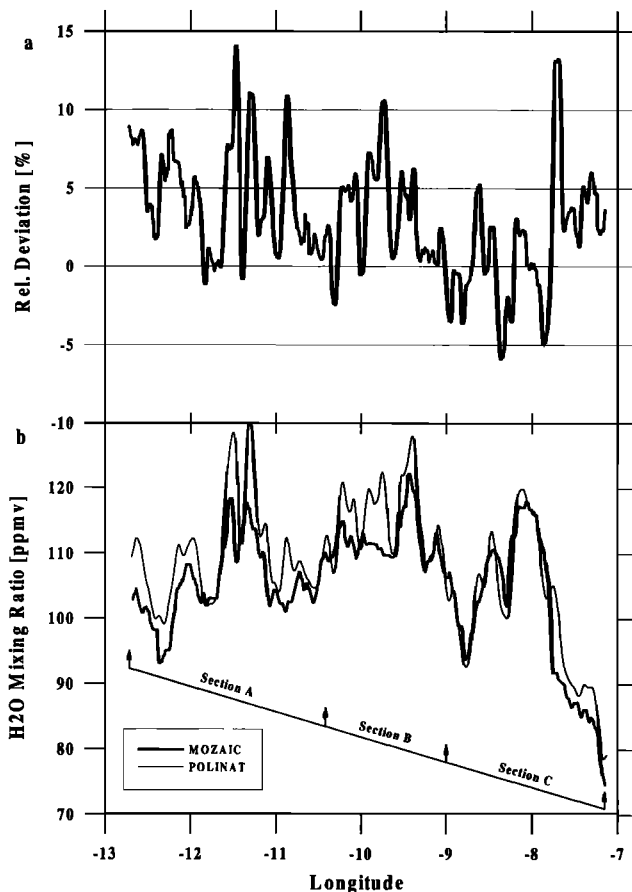


Figure 9. MOZAIC and POLINAT water vapor volume mixing ratios as a function of longitude. The MOZAIC measurement is shifted by 15 s opposite to the flight direction. Figure 9a shows the relative differences $(\text{POLINAT}-\text{MOZAIC})/\text{MOZAIC}$ in percent.

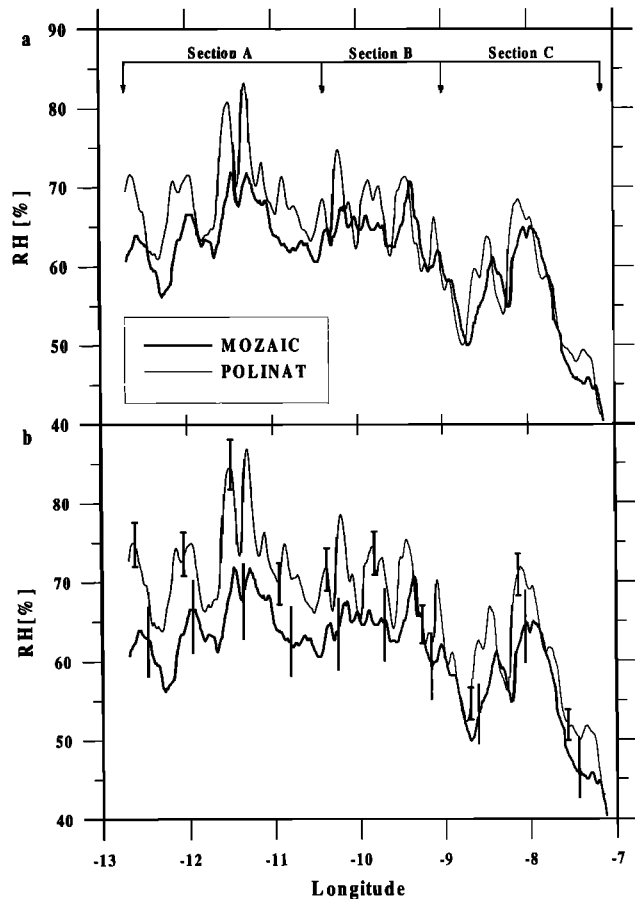


Figure 10. MOZAIC and POLINAT relative humidity (RH) as a function of longitude. (a) RH of POLINAT is computed using the temperature measured with the POLINAT PT100 sensor. (b) RH of POLINAT is computed using the temperature measured with the POLINAT PT500 sensor. The uncertainties of both measurements are plotted as error bars in Figure 10b.

-55°C and 59.9% for -52°C), in particular, before reaching -8° longitude, as was to be expected from the observed long-lasting contrail (Plate 1). The POLINAT data show systematically higher values than the MOZAIC measurement. One has to be aware that RH is the parameter measured with the MOZAIC sensor directly (though corrected for the difference between conditions at the sensor and in the ambient air, as a function of SAT , TRT , and P , using (2)), but in the case of the POLINAT data, RH has to be derived from the POLINAT volume mixing ratio measurement by (7), which includes two additional measured parameters SAT and P with their respective uncertainties. POLINAT selected the SAT measurement of the PT500 (which is the slower but more stable sensor and hence usually the more accurate probe compared to the PT100) for the derivation of the relative humidity. This temperature sensor showed the lowest temperature compared to the measurements of three other sensors (Figure 6). Selecting the POLINAT measurement with the PT 100, which is closest to the MOZAIC temperature, for the computation of the POLINAT RH leads to an excellent agreement ($\pm 5\%$) of both measurements (Figure 10a). One recognizes here the strong dependence of RH on temperature. This strong temperature dependence also comes into play by the computation of $\mu_{\text{H}_2\text{O}}$ from the MOZAIC RH measurement by (4) through the factor $E(SAT)$ in the formula.

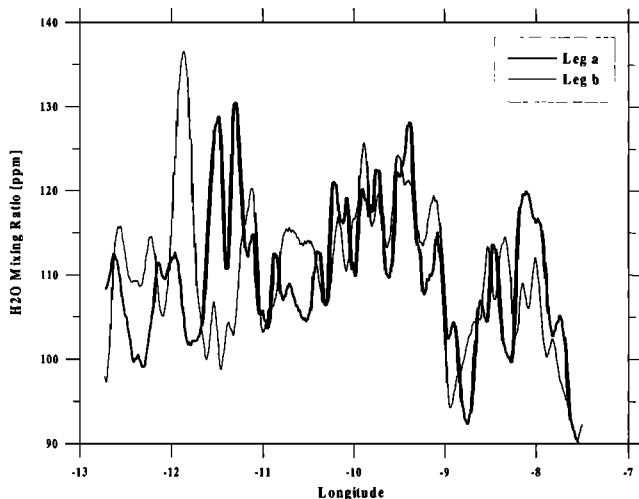


Figure 11. POLINAT water vapor volume mixing ratio as a function of longitude measured on flight legs a and b.

For section C, where both aircraft sampled nearly the same air parcels, the measurements are in good agreement; even single features of RH are resolved by both instruments. The uncertainty of RH for the POLINAT measurements is again larger here than for the volume mixing ratio because in (7), SAT and P add considerably to the uncertainty of μ_{H_2O} .

The POLINAT aircraft also executed a back flight on its own track, flight leg b (Figure 2). The water vapor mixing ratio on this route shows a fair overall agreement between -7° and -11° longitude (Figure 11). In spite of slight deviations of the flight paths in the two sections and changes in the state of the atmosphere with time during the flights, the data, in particular in the period of best agreement between the flight paths and early times, between -9° and -10° , show that the mixing ratio measurements are easily reproduced. The time lag between legs a and b of the *FALCON* varied from 2.5 to 61 min between -7° and -11° longitude. In addition, the wind increased appreciably between both flight legs (Figure 4), so that the structure of the water vapor distribution met on leg a changed more and more with the time lag between leg a and b. This demonstrates that only very small differences in distance and time can give conclusive information in comparisons of atmospheric water vapor measurements. The data of the intercomparison flight of both aircraft were first sent to A. Marengo for a quick look intercomparison and have not been changed.

5. Conclusions

A comparison of water vapor measurements on a MOZAIC and a POLINAT flight was performed in order to evaluate the quality of the water vapor measurements of both projects. Two completely different techniques of water vapor measurement were employed. POLINAT uses a cryogenic frost-point instrument, a primary standard instrument for the measurement of the frost-point temperature of ambient air. The MOZAIC device is a hydroactive polymer sensor that measures relative humidity (dynamic relative humidity (RH_D)) inside a Rosemount 102 BX sensor housing. The relative humidity of the ambient air (RH_S) is deduced from RH_D by using the measured temperature of the adiabatically heated air, pressure, and speed of the aircraft. The

water vapor volume mixing ratio is deduced from the measured relative humidity, ambient pressure, static air temperature, and total recovery temperature. MOZAIC sensors are individually calibrated in the laboratory at regular intervals, before and after flight periods of 4 weeks, against a laboratory Lyman α fluorescence hygrometer. POLINAT measures frost-point temperature, and the water vapor mixing ratio is determined from frost-point temperature and air pressure without further input.

The water vapor mixing ratios that were derived from these two different and independent instruments differ by $<\pm 5\%$ for section C, the period of closest approach of flight routes of the aircraft. The uncertainties of both measurement techniques are well documented and explicitly given for this intercomparison flight.

Relative humidities from MOZAIC and POLINAT agreed to within 15%, which is within the combined errors of the two methods. This lesser agreement could be caused by the PT500 temperature measurement used by POLINAT for the RH determination, which deviates systematically from two MOZAIC and one additional POLINAT temperature measurements. Although all four temperature measurements show agreement within the quoted uncertainty of $\pm 0.5^\circ\text{C}$, the RH variation with temperature is so strong that a small bias between the POLINAT PT500 temperature measurement, compared to the other three temperature measurements, causes practically all of the differences between the POLINAT and MOZAIC RH values. Conversely, if the temperature measured by the POLINAT PT100 sensor is used, the RH agreement is within 5%, as good as for the determination of the water vapor mixing ratio.

The measurements were performed at temperatures between -55° and -53°C and at ambient humidity values between 40 and 80%, near and partly above ice saturation. Lower ambient temperatures and lower ambient humidity values would have provided more stringent test conditions.

The MOZAIC – POLINAT comparison was undertaken to validate the MOZAIC instrumentation in flight against the frost-point hygrometer as a standard instrument that works on first principles. Since relative humidity and mixing ratio from MOZAIC and POLINAT agree to within 5%, it is therefore demonstrated that over the comparison range above 80 ppm, MOZAIC measures upper tropospheric relative humidity and water vapor mixing ratio with an absolute overall accuracy similar to that of the frost-point hygrometer sensor on the POLINAT aircraft.

Since the MOZAIC hygrometer is regularly calibrated in the laboratory against a Lyman α fluorescence hygrometer [Kley and Stone, 1978], it also appears that the POLINAT frost-point hygrometer and the Lyman α fluorescence hygrometer, intermediated through the MOZAIC relative humidity sensor, agree to within 5% for water vapor mixing ratios of 80–120 ppm.

POLINAT data have been used to validate humidity models for numerical analysis of meteorological fields and weather prediction [Ovarlez and Velthoven, 1997]. The MOZAIC project has resulted in a large set of humidity data at the flight routes of aircraft that has been evaluated in a parallel study to determine the frequency of ice supersaturation in the upper troposphere and lower stratosphere [Gierens et al., 1999]. Because of its good accuracy and quasi-global coverage, the MOZAIC water vapor data set can be used for the evaluation of water vapor satellite instruments for applications in the upper troposphere.

Acknowledgments. We thank Air France, Austrian Airlines, Lufthansa, and Sabena for carrying the MOZAIC equipment on scheduled

flights and handling regular installation/deinstallation of the sensors. We acknowledge with gratitude the strong support of Airbus Industry and partners. We sincerely thank the European Commission (DG XII-C: Aeronautics and DG XII-D: Environmental Program) for funding our work in the MOZAIC I and II and the POLINAT 1 and 2 projects. Support by the Shannon Air Traffic Control is gratefully acknowledged. We thank the *Falcon* flight and ground crew of DLR for expert flight operations and H. Ovarlez and his team at LMD for the frost-point hygrometer development and operation.

References

- Elliott, W. P., and D. J. Gaffen, On the utility of radiosonde humidity archives for climate studies, *Bull. Am. Meteorol. Soc.*, **72**, 1507-1520, 1991.
- Gierens, K., U. Schumann, H. G. J. Smit, M. Helten, and G. Zangl, Determination of humidity and temperature fluctuations based on MOZAIC data and parameterisation of persistent contrail coverage for general circulation models, *Ann. Geophys.*, **15**, 1057-1066, 1997.
- Gierens, K., U. Schumann, M. Helten, H. G. J. Smit, and A. Marengo, A distribution law for relative humidity in the upper troposphere and lower stratosphere derived from three years of MOZAIC measurements, *Ann. Geophys.*, in press, 1999.
- Goff, J. A., and S. Gratch, Low-pressure properties of water from -160 to 212 F, *Trans. Am. Soc. Heat. Vent. Eng.*, **52**, 95-122, 1946.
- Harriss, J. E., Atmospheric radiation and atmospheric humidity, *Q. J. R. Meteorol. Soc.*, **123**, 2173-2186, 1997.
- Helten, M., H. G. J. Smit, W. Sträter, D. Kley, P. Nedelec, M. Zöger, and R. Busen, Calibration and performance of automatic compact instrumentation for the measurement of relative humidity from passenger aircraft, *J. Geophys. Res.*, **103**, 25,643-25,652, 1998.
- Houghton, J. T., L. G. Meira Filho, B. A. Callander, N. Harris, A. Kattenberg, and K. Maskell, *Climate Change 1995: The Science of Climate Change*, Intergov. Panel of Clim. Change, Cambridge Univ. Press, New York, 1996.
- Kiehl, J. T., and K. E. Trenberth, Earth's annual global mean energy budget, *Bull. Am. Meteorol. Soc.*, **78**, 197-208, 1997.
- Kley, D., Ly(a) absorption cross section of H₂O and O₂, *J. Atmos. Chem.*, **2**, 203-210, 1984.
- Kley, D., and E. J. Stone, The measurement of water vapor in the stratosphere by photodissociation with Ly (1216 Å) light, *Rev. Sci. Instrum.*, **49**, 691-697, 1978.
- Leiterer, U., H. Dier, and T. Naebert, Improvements in radiosonde humidity profiles using RS80/RS90 radiosondes of Vaisala, *Contrib. Atmos. Phys.*, **70**, 319-336, 1997.
- Manabe, S., and R. Wetherald, Thermal equilibrium of the atmosphere with a given distribution of relative humidity, *J. Atmos. Sci.*, **24**, 241-259, 1967.
- Marengo, A., et al., Measurement of ozone and water vapor by AIRBUS in-service aircraft: The MOZAIC airborne program, an overview, *J. Geophys. Res.*, **103**, 25,631-25,642, 1998.
- Möller, F., On the influence of changes in the CO₂ concentration in air on the radiation balance of the Earth's surface and on the climate, *J. Geophys. Res.*, **68**, 3877-3886, 1963.
- Oltmans, S. J., Measurements of water vapor in the stratosphere with a frost-point hygrometer, in *Moisture Humidity*, pp 251-258, Instrum. Soc. of Am., Research Triangle Park, N. C., 1985.
- Ovarlez, J., Stratospheric water vapor measurement in the tropical zone by means of a frost point hygrometer on board long-duration balloons, *J. Geophys. Res.*, **96**, 15,541-15,545, 1991.
- Ovarlez, J., and P. van Velthoven, Comparison of water vapor measurements with data retrieved from ECMWF analyses during the POLINAT experiment, *J. Appl. Meteorol.*, **36**, 1329-1335, 1997.
- Quante, M., P. R. A. Brown, R. Baumann, B. Guillemet, and P. Hignett, Three-aircraft intercomparison of dynamical and thermodynamical measurements during the Pre-EUREX campaign, *Contrib. Atmos. Phys.*, **69**, 129-146, 1996.
- Schlager, H., P. Konopka, P. Schulte, U. Schumann, H. Ziereis, F. Arnold, M. Klemm, D. E. Hagen, P. D. Whitefield, and J. Ovarlez, In situ observations of air traffic emission signatures in the North Atlantic flight corridor, *J. Geophys. Res.*, **102**, 10,739-10,750, 1997.
- Schumann, U., On conditions for contrail formation from aircraft exhausts, *Meteorol. Z.*, **5**, 4-23, 1996.
- Schumann, U. (Ed.), Pollution from aircraft emissions in the North Atlantic flight corridor (POLINAT), *Air Pollut. Res. Rep. 58, Rep. EUR 16978 EN*, 303 pp., Off. for Off. Publ. of the Eur. Communities, Luxembourg, Luxembourg, 1997.
- Schumann, U., H. Schlager, F. Arnold, R. Baumann, P. Hascherberger, and O. Klemm, Dilution of aircraft exhaust plumes at cruise altitudes, *Atmos. Environ.*, **32**, 3097-3103, 1998.
- Shine, K. P., and A. Sinha, Sensitivity of the Earth's climate to height-dependent changes in the water vapor mixing ratio, *Nature*, **354**, 382-384, 1991.
- Sonntag, D., Advancements in the field of hygrometry, *Meteorol. Z.*, **3**, 51-66, 1994.
- Ström, J., R. Busen, M. Quante, B. Guillemet, P. R. A. Brown, and J. Heintzenberg, Pre-EUCREX intercomparison of airborne humidity measuring instruments, *J. Atmos. Oceanic Technol.*, **11**, 1392-1399, 1994.
- World Meteorological Organization (WMO), Measurement of atmospheric humidity, in *Guide to Meteorological Instruments and Methods of Observation*, 5th ed., *WMO Rep. 8*, pp. 5.1-5.19, Geneva, 1983.
- R. Baumann, H. Schlager, and U. Schumann, Institut für Physik der Atmosphäre, Deutsches Zentrum für Luft- und Raumfahrt, Oberpfaffenhofen, D-82234 Wessling, Germany. (robert.baumann@dlr.de; hans.schlager@dlr.de; ulrich.schumann@dlr.de)
- M. Helten, D. Kley, and H. G. J. Smit, Institut für Chemie der Belasteten Atmosphäre, Forschungszentrum Jülich, D-52425 Jülich, Germany. (m.helten@fz-juelich.de; d.kley@fz-juelich.de; h.smit@fz-juelich.de)
- A. Marengo and P. Nedelec, Laboratoire de'Aérodologie, CNRS, 14 Avenue Edouard Belin, F-31400 Toulouse, France. (mara@aero.obs-mip.fr; nedp@aero.obs-mip.fr)
- J. Ovarlez, Laboratoire de Météorologie Dynamique du CNRS (LMD), Ecole Polytechnique, F-91128 Palaiseau cedex, France. (joelle.ovarlez@polytechnique.fr)

(Received January 6, 1999; revised May 3, 1999; accepted May 6, 1999.)